New Energy Management System for RES-based Microgrid Operations using SGO

MADHAB CHANDRA DAS[1], PRITAM PATEL[1], SARAT CHANDRA SWAIN[1],
BINAY KUMAR NAYAK[2]
[1]KIIT University,
Bhubaneswar,
INDIA

[2]Indira Gandhi Institute of Technology,
Sarang,
INDIA

Abstract: - Due to advantages such as abundant energy sources, environmentally friendly perspectives, and straightforward power extraction, there has been increasing research on integrated microgrids incorporating photovoltaic (PV), wind, and biogas systems. Efficient utilization of renewable energy sources (RES), backup distributed generators (DGs), and storage devices within the microgrid is essential to meet power demands. Consequently, Energy Management Systems (EMS) have been introduced to microgrids, focusing on monitoring various energy resources and regulating energy consumption at specific locations. In this manner, the EMS effectively coordinates the integrated DGs within the microgrid to ensure optimal power supply to loads with minimal operational costs. The aid of decision-makers lies in comprehending a location's strengths and constraints, enabling them to regulate usage effectively. To enhance productivity, all potential distributed generators (DGs) must be integrated into the microgrid and optimized. Despite numerous global research efforts in devising energy management systems, certain challenges persist. Ensuring a microgrid provides reliable, high-quality power is demanding, primarily due to geographical dispersion, restricted availability of distributed resources, and the seasonal and intra-day variability inherent in renewable resources. Managing a microgrid becomes intricate given these factors.

Key-Words: - Microgrid; renewable energy; energy management; energy storage; distributed generation; Social group optimization; HOMER Pro software.

Received: September 12, 2023. Revised: July 9, 2024. Accepted: August 11, 2024. Published: September 27, 2024.

1 Introduction

A microgrid is a small-scale power-generating system that supplies the electricity needed locally. The first microgrid in the United States was a 64 MW plant built at the Whitling Refinery in Indiana in 1955, according to [1], however, the idea behind microgrids dates back much further. Beginning in the late 1700s, the microgrid idea uses a tiny local power generating system to fulfill demand measured in kilowatt-hours. A decentralized power production and storage system, able to balance supply and demand and provide dependable service within its boundaries, should be a feature of every conventional microgrid. Although there isn't a set minimum or maximum size for a microgrid, it should be big enough for a small town, such as a hospital, school, university, or military base. However, a single-generation system, often known as a nano-grid, is any power production system that supplies a single building, whether it is commercial, industrial, or residential, [2]. The initial goals of the microgrid idea were to address energy scarcity, improve the integration of distributed renewable energy sources, and reduce the environmental impacts of traditional power production systems, such as greenhouse gas emissions and carbon footprint. Electrifying rural areas, effectively integrating Distributed Generation (DG), and relieving pressure on the transmission and distribution systems by producing electricity where it is required are other incentives, [3], [4]. By offering an efficient platform for integrating and monitoring the DG sources, microgrids may be defined as the conversion of the conventional power generating system into a more dependable, less carbon-intensive, and cost-effective energy system. Being a scaled-down version of the main grid, the microgrid also offers closer proximity between the source and consumption of electricity, increasing efficiency and lowering transmission losses. Renewable energy sources including solar, wind, small hydro, geothermal, waste-to-energy, and combined heat and power systems can all be integrated into a microgrid. Based on how they operate, microgrid technologies may be divided into two categories: (i) stand-alone or decentralized modes, and (ii) grid-connected or centralized modes [5], [6]. The goal of this research project is to assess the local potential of renewable energy sources, such as solar and wind power, and to suggest an integrated energy management system that would enable microgrid operations to be highly reliable and low-maintenance. To achieve this, the following objectives are defined:

I. Using the meteorological information that is currently available, create a model for mapping and forecasting the local potential for solar and wind energy.
II. Estimate ideal land available in the regions with higher renewable energy potential for the installation of solar fields and wind farms and develop a generalized methodology for solar field and wind farm layout to maximize the power generation.
III. Investigate an integrated renewable energy system for stand-alone microgrid operations.

The goal of this paper is to design an energy management system that takes into account locally accessible renewable energy sources for microgrid operations at the local scale. The goal of microgrid development is to reduce greenhouse gas emissions while meeting the energy needs of the present and the future with high dependability and minimal cost in [7], [8]. The paper defines the process for accurately assess the potential for renewable energy, settling the best location for installing an energy system, and maximize the use of available energy resources. A new area is select for the arrangement of IRES, and the method used in this study can also be applied to other locations with locally acquirable renewable energy resources and energy desire.

2 Microgrid Architecture

2.1 System Configuration

An endeavor has been created to model Photovoltaic Solar and Wind Power as Distributed Generation power sources with energy storage system are interconnected to the grid in Figure 1 and the system is tested through the HOMER pro software. This software simplifies the examination of multiple configurations of the whole system, considering different capacities for each component. These configurations were appraised to determine their capability to execute the load requirements. The HOMER Pro software was employed to generate a list of viable configurations capable of meeting the demand, which were then organized based on economic indicators such as the Levelized Cost of Energy (LCOE) and Net Present Cost (NPC).

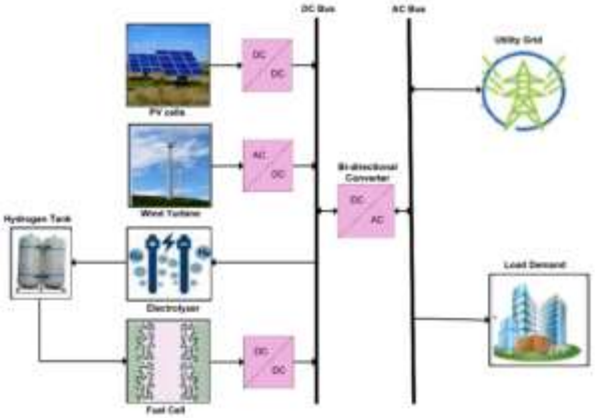

Fig. 1: Proposed microgrid with control system

2.2 Modelling Of Photovoltaic System

The calculation for the AC output of a photovoltaic panel be expressed as follows:

$$P_{PV}(t) = A \times \eta \times N_{PV} \times Irr(t) \times \eta_{inv} \times f_{temp} \quad (1)$$

where A denotes the panel's area, η denotes panel efficiency, Irr stands for global horizontal irradiance (GHI) expressed in W/m2, and η_{inv} stands for inverter efficiency. is the derating factor caused by the temperature that modifies the output power of a PV panel. It's computed as

$$f_{temp} = [1 - \alpha(\Gamma - T_{ref})] \quad (2)$$

where, Γ is the module temperature which is calculated as

$$\Gamma = T + 0.035 Irr(t) \tag{3}$$

where T is the atmospheric temperature.

The monthly predicted solar radiation was compared with the measured values and plotted for two test locations (T1) and (T2) in Figure 2. The result indicates better fitting of value, and prediction for each month is very near to actual value for all test locations.

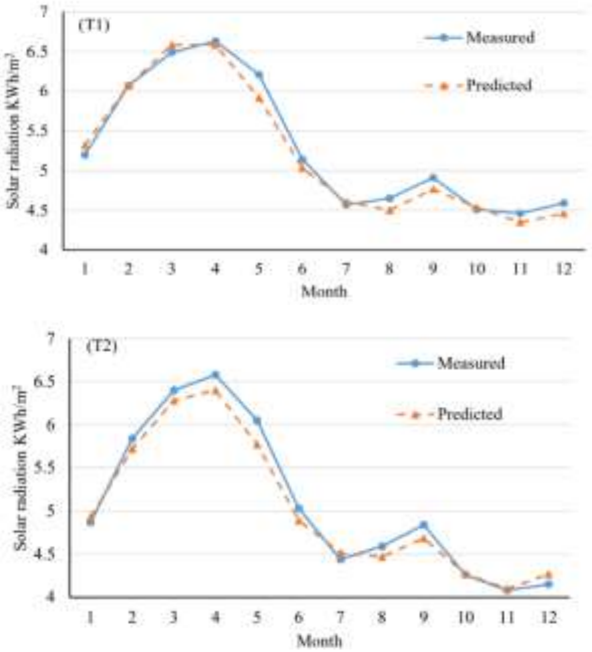

Fig. 2: Comparison between measured values and predicted values of solar radiation for two test locations (T1) and (T2) in a year

2.3 Modelling Of Wind System

Temperature, pressure, and relative humidity are the three meteorological characteristics that have been considered in order to examine the impact of various components on wind speed prediction.

$$P_{\text{wind}}=0.5\cdot\rho\cdot A\cdot C_p\cdot V_3 \tag{4}$$

Where A is the swept area of the wind turbine blades, V is the wind speed, Cp is the power coefficient, which indicates the turbine's efficiency, and Pwind is the power taken from the wind.

Figure 3(a) and Figure 3(b) represented measured and predicted value of wind speed for two test locations (T1) and (T2). The result shows a closer approximation between measured and predicted values of wind speed. As it can be seen in the Figure 3(a) the predicted values of wind speed follow the trend and are reasonably close to the measured values of wind speed.

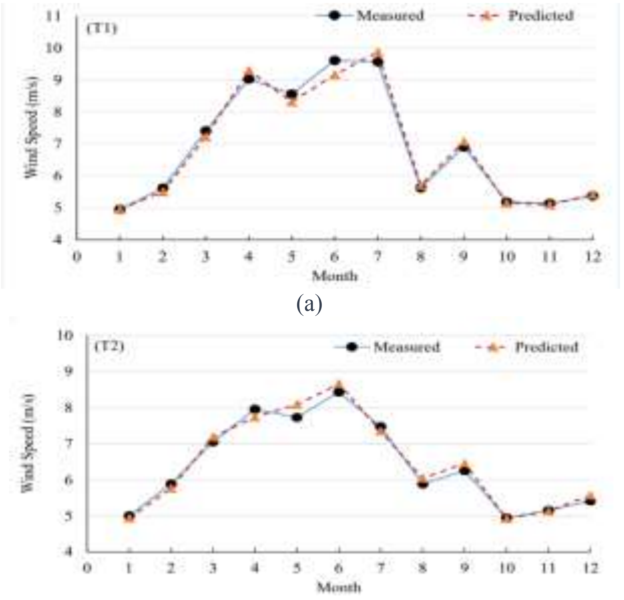

(a)

(b)

Fig. 3: Comparison of measured values and predicted values of wind speed for two test locations (T1) and (T2) in a year

The analysis focuses on wind turbines with a capacity of 3 kW from Diamond Engineering Enterprises, India, characterized by a capital cost of Rs. 50,000/-. The predicted monthly mean wind speed is based on the methodology. Power generation profile of a chosen wind turbine is shown in Figure 4.

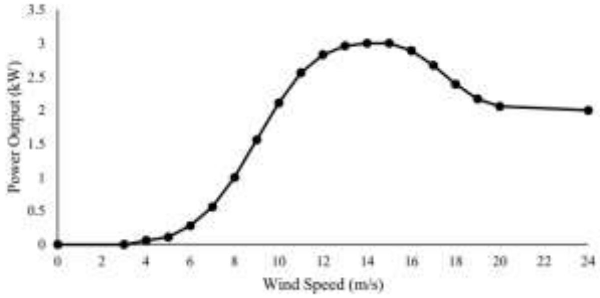

Fig. 4: Power output Vs wind speed

2.4 Modelling Of Battery Energy Storage System (Bess)

For the battery bank in our investigation, we use gelled electrolyte-sealed batteries, a particular kind of valve-regulated lead-acid (VRLA) battery. There is a connection between the PV panel's output power, the load demand at time t, and the battery bank's state at hour t. A valve is built into every VRLA battery cell to keep airborne oxygen out and let out any gas produced during overcharging. Lead acid-sealed batteries are another name for these VRLA batteries. In [9], [10], [11] configuration, batteries are connected in both series and parallel to establish the battery bank. The total number of batteries is determined by an Equation which accounts for the arrangement of 83 batteries in series and 48 batteries in parallel.

Every hour, the battery's charge state is updated by the power that is being charged and discharged. Equation of charge:

$$SOC(t) = SOC(t-1) \times (1-\sigma) + \eta_{ch} \frac{P_{bat}(t)}{C_{bat} \times V} \tag{5}$$

$$SOC(t) = SOC(t-1) \times (1-\sigma) - \eta_{dch} \frac{P_{bat}(t)}{C_{bat} \times V} \tag{6}$$

SOC(t) and *SOC (t -1)* are the state of charge of the battery at hour (t) and (t -1), respectively, C_{bat} = the capacity of the battery at hour t hour,

$$N_b = N_S \times N_P \tag{7}$$

Ns is the number of batteries in series, N_P is the number of batteries in parallel, and N_b is the total number of batteries.

V is the nominal battery voltage, σ is the discharging factor (2.8%) per month, η_{ch} is the charging efficiency (97%), and η_{dch} is the discharging efficiency (94%). The battery power exchanged during the simulation is plotted in Figure 5.

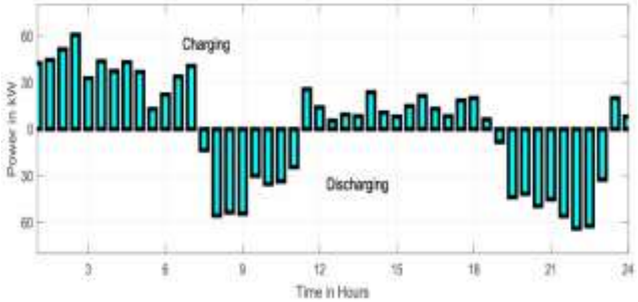

Fig. 5: Power exchange from the battery

2.5 Modelling Of Load

The monthly average electrical energy demand of khordha village, is presented in Figure 6(a). Also, Figure 6(b) shows the hourly load profile for June, which has the maximum energy demand in the year. To develop and analyze IRES at the study location, the electrical energy demand of 100 households along with the energy demand at a medical center and a school is considered, which have an approximate yearly energy demand of 317 MWh.

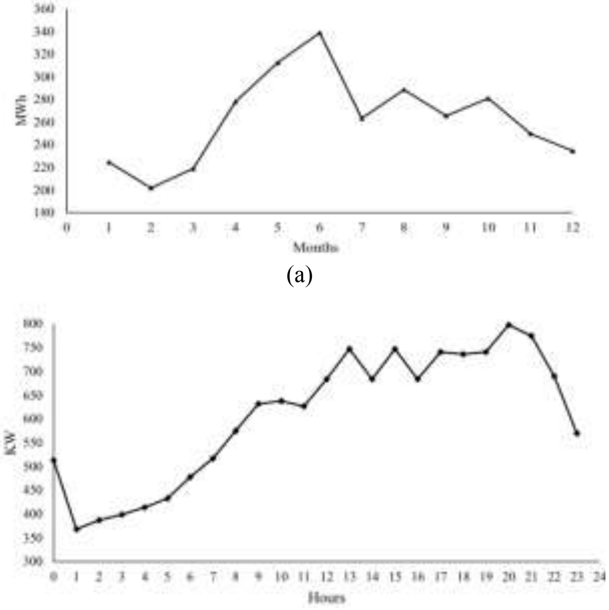

(a)

(b)

Fig. 6: Annual and hourly load profile for Khordha district (2023)

3 Energy Management System

To reduce the cost of the energy supply in both modes of operation, the ideal combination of power generation from various generating sources is required. Energy management systems handle the ideal blend of power generation (EMS). To guarantee the dependability of the energy supply, the EMS advises the operator on how to use the system power efficiently. It is a supply-demand balance, which forms an optimization problem. When this problem considers real-world constraints, rather than just an abstract mathematical function, it becomes more complex, [12]. The size of the microgrid varies with applications, however, it is designed/operationalized to match the supply 13 demand requirements. For efficient implementation of EMS, it would be beneficial to have a unified communication interface. In [13], [14], A typical approach adopted in the sizing of energy management systems is presented in Figure 7.

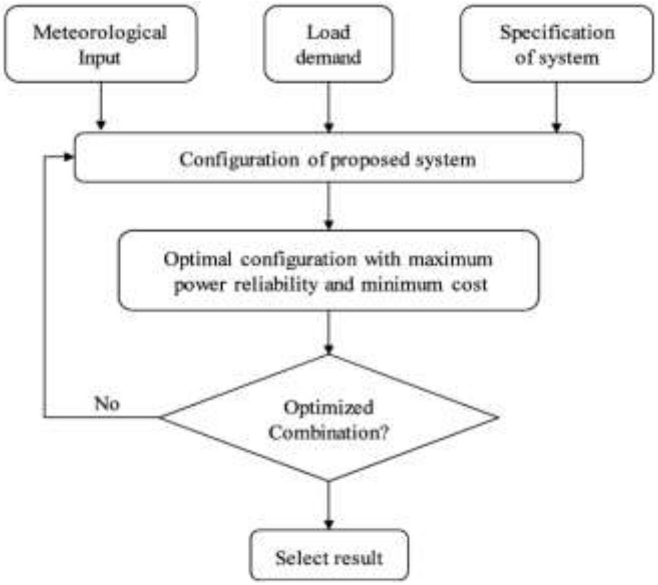

Fig. 7: Typical approach adopted in sizing of energy management systems

4 Problem Formulation

The innovative energy management system assists in assessing the viability of each scenario through the implementation of an economic analysis. This analysis encompasses economic factors, including the Levelized Cost of Electricity (LCOE) and Net Present Cost (NPC) in [15], [16]. The LCOE is computed using Equation (8) in units of Rs/kWh.

$$LCOE = \frac{(Cann,total - Cboiler\ Hserved)}{Eserved} \tag{8}$$

In this context, where C_{ann}, the total represents the total annual cost (Rs/yr.), C_{boiler} signifies the marginal cost of the boiler (Rs/kWh), H_{served} stands for the overall thermal load served (kWh/yr.), and E_{served} denotes the total electrical load (kWh/yr.). Our study employs the Social Group Optimization technique to identify optimal solutions, maximizing the objective function, as outlined in [17], [18]. The objective function in this case is the analysis of the financial benefits associated with Integrated Renewable Energy Systems (IRES).

$$f_{obj} = \max(CB) \tag{9}$$

where *CB* is the financial benefit which can be calculated as follows:

$$CB = \sum_{d=1}^{365} \sum_{t=1}^{24} benf(d,t) \tag{10}$$

$$benf(d,t) = price(d,t) \times P_{grid}(d,t) \tag{11}$$

where *benf* is the hourly financial benefit, P_{grid} is the hourly power transacted between the utility grid and the microgrid.

5 Simulation Results

Hourly solar irradiation data for the year 2023-24 in Khordha, Odisha, serves as the input for the simulation. The MATLAB platform is utilized for conducting the simulation. To address the optimization problem, a Single-Objective Social Group Optimization (SGO) algorithm has been applied. The parameters of the SGO algorithm are detailed in Table 1.

Table 1. Parameters of Sgo

Dimension of the problem, D	50
Population Size, N	50
Maximum Iteration, $iter_{max}$	270
Limit	[0,20]
Self-introspection parameter, c	0.26

5.1 Comparison of Scenarios and IRES Analysis

Figure 8 depicts the comparison of the optimal choices in each scenario concerning Net Present Cost (NPC) and Initial Capital Cost (ICC). Meanwhile, Figure 9 provides a comparison of the Levelized Cost of Electricity (LCOE) among all considered scenarios, each representing the best combination.

Scenario A: wind + diesel + li-ion battery + AC-DC
Scenario B: PV + diesel + li-ion battery + AC-DC
Scenario C: PV + wind + li-ion battery + AC-DC
Scenario D: wind + fuel cell + electrolyzer + hydrogen tank + DC-AC
Scenario E: PV + fuel cell + electrolyzer + hydrogen Tank + DC-AC
Scenario F: Biogas generator
Scenario G: PV + wind + li-ion battery + diesel+ biogas + DC-AC

In Scenario A, where wind turbines are utilized, both LCOE and NPC experience an increase due to the turbine's dependency on favorable wind conditions, rendering them ineffective during low wind speeds. Conversely, Scenario B exhibits lower LCOE and NPC values, attributed to the greater reliability of PV panels and the reduced variability in solar radiation compared to wind speed in

Bhubaneswar, Odisha. In Scenario C, where a combination of wind turbines and PV panels is employed, there is a slight increase in LCOE and NPC. Scenarios D and E introduce fuel cells alongside wind and PV systems, resulting in considerably higher LCOE and NPC values. This is attributed to fuel cell technology being relatively new and necessitating further development as an alternative solution. Thus, these scenarios (D and E) are regarded as futuristic. Scenario F, featuring a biogas generator, emerges as a promising energy resource, displaying the lowest ICC among all scenarios. However, due to limited resources, the biogas generator falls short of meeting the total energy demand. Scenario G (Integrated Renewable Energy System - IRES), which integrates various renewable energy sources into a microgrid, boasts the lowest LCOE and NPC. Figure 8 illustrates the contribution of different renewable energy sources in meeting energy demands, with 85% met by PV panels, followed by 11% and 4% from biogas generators and wind turbines, respectively. This underscores that the PV system is the most economical and feasible option for power generation in the Khordha district.

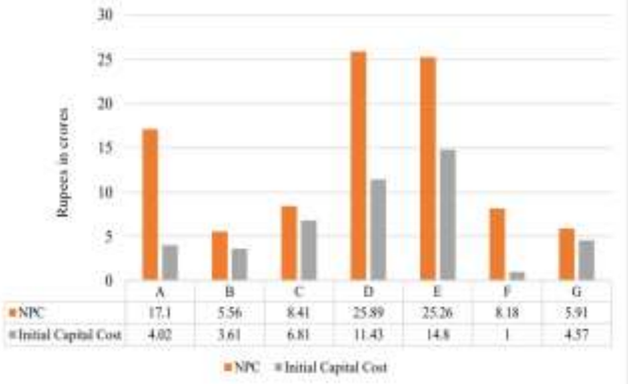

Fig. 8: Comparison of all scenarios based on NPC and ICC

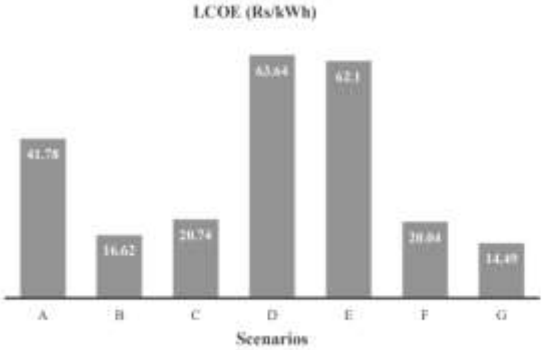

Fig. 9: Comparison of LCOE in all scenarios

Scenario 'C in Figure 8 and Figure 9 was devised to examine the feasibility of meeting electrical demand solely through the combination of PV and wind with a battery, excluding the use of a diesel generator. This configuration utilizes both wind and PV, resulting in a renewable energy fraction of 100%. However, the LCOE for this scenario stands at Rs. 20.75, which is comparable. Still, it has an NPC of Rs. 8.41 crores and an ICC of Rs. 6.81 crores, rendering it economically less competitive.

5.2 RES for Microgrid Operation

An Integrated Renewable Energy System (IRES) was developed for a microgrid system to fulfill the electrical demand of Khordha village, focusing on the energy requirements of 100 existing houses. The analysis incorporated various energy generation units, including photovoltaic (PV), wind, and biogas, coupled with energy storage units such as batteries. Seven scenarios, encompassing both realistic and futuristic options, were formulated with diverse combinations of energy sources and storage systems in Table 2. These scenarios were assessed using HOMER Pro software, considering their Levelized Cost of Energy (LCOE) and Net Present Cost (NPC). The futuristic scenarios involved Valve-Regulated Lead-Acid (VRLA) batteries in conjunction with wind and/or solar generation systems. The optimal futuristic scenario exhibited a maximum LCOE of 63.64 Rs. /kWh. In contrast, the realistic scenarios utilized PV, solar, wind, and biogas as generation systems, with the lowest LCOE recorded at 14.49 Rs. /kWh, as depicted in Figure 9.

Table 2. Analysis of Different Scenarios

Scenarios	COE (Rs/kWh)	NPC (Cr. Rs)	ICC (Cr. Rs)	RE (%)
A	41.78	17.10	1.10	27.39
B	16.62	5.56	3.61	87.32
C	20.74	8.41	6.81	100
D	63.64	25.89	11.43	23.64
E	62.1	25.26	14.8	39.8
F	20.04	8.18	1	100
G	14.49	5.91	4.57	100

6 Conclusion

The study underscores the cost-effective power generation aspect, indicating that the optimal number of wind turbines decreases with an increase in wind speed for a given size of the wind farm. Furthermore, a 30 m x 40 m solar field in Khordha district can generate 1.2 MWh/day with an average solar radiation of 5.26 kWh/m²/day, capable of meeting the energy demand of 100 households. In the investigation of seven different Integrated Renewable Energy System (IRES) scenarios, it is determined that the IRES combining PV, wind, and biogas achieves a Levelized Cost of Electricity (LCOE) of 14.46 Rs/kWh without subsidies or policy interventions. The feasibility analysis, considering policy interventions and carbon abatement costs, results in a reduced LCOE of 8.6 Rs/kWh, establishing it as a sustainable option for the study region. The application of Social Group Optimization (SGO) is proven to be a fast, efficient, and reliable method for solving the optimization problem.

References:

[1] Achilles, S., Alvarez-Cordero, G., Apostolov, A., Avramidis, I., Bachiller-Soler, A., Badrzadeh, B., ... & Bose, A. 2023 Index *IEEE Power and Energy Magazine* Vol. 21.

[2] Kassem, Y., Gokcekus, H., Hamad, O. A. M., & Fayid, F. M. B. (2023). Economic viability of a 6.5 kW off-grid solar PV with various sun-tracking systems in Northern Cyprus: A case study. *Engineering, Technology & Applied Science Research*, 13(2), 10608-10621.

[3] Gholami, M., Muyeen, S. M., & Lin, S. (2024). Optimizing microgrid efficiency: Coordinating commercial and residential demand patterns with shared battery energy storage. *Journal of Energy Storage*, 88, 111485.

[4] Agajie, T. F., Ali, A., Fopah-Lele, A., Amoussou, I., Khan, B., Velasco, C. L. R., & Tanyi, E. (2023). A comprehensive review on techno-economic analysis and optimal sizing of hybrid renewable energy sources with energy storage systems. *Energies*, 16(2), 642.

[5] El-Houari, H., Allouhi, A., Salameh, T., Kousksou, T., Jamil, A., & El Amrani, B. (2021). Energy, Economic, Environment (3E) analysis of WT-PV-Battery autonomous hybrid power plants in climatically varying regions. *Sustainable Energy Technologies and Assessments*, 43, 100961.

[6] Mishra, S., Pattanaik, D., Pau, R., Dash, R., & Swain, S. C. (2018, October). A Review on Different Types of Maximum Power Point Tracking System & its Application with PR Current Control Technique. In *2018 International Conference on Applied Electromagnetics, Signal Processing and Communication (AESPC)* (Vol. 1, pp. 1-6). IEEE.

[7] Merabet, A., Qin, Z., & Ghias, A. M. (2018, October). Control of simulated solar PV microgrid operating in grid-tied and islanded modes. In *IECON 2018-44th Annual Conference of the IEEE Industrial Electronics Society* (pp. 1729-1734). IEEE.

[8] Swain, S. C., Gogoi, A., Sharma, S., Dash, R., & Acharya, A. (2018, July). Some aspects of fuzzy logic controller for designing MPPT based SPV system. In *2018 International Conference on Recent Innovations in Electrical, Electronics & Communication Engineering (ICRIEECE)* (pp. 3357-3361). IEEE.

[9] Ren, H., Zhao, Y., Chen, S., & Wang, T. (2019). Design and implementation of a battery management system with active charge balance based on the SOC and SOH online estimation. *Energy*, 166, 908-917.

[10] Chen, Yu-Kai, et al. "Design and implementation of energy management system with fuzzy control for DC microgrid systems." *IEEE Transactions on Power Electronics,* 28.4 (2012): 1563-1570.

[11] Merabet, A., Al-Durra, A., & El-Saadany, E. F. (2022). Energy management system for optimal cost and storage utilization of renewable hybrid energy microgrid. *Energy Conversion and Management*, 252, 115116.

[12] Ibrahim, O., Bakare, M. S., Amosa, T. I., Otuoze, A. O., Owonikoko, W. O., Ali, E. M., & Ogunbiyi, O. (2023). Development of fuzzy logic-based demand-side energy management system for hybrid energy sources. E*nergy Conversion and Management*: X, 18, 100354.

[13] Ullah, Z., Wang, S., Lai, J., Azam, M., Badshah, F., Wu, G., & Elkadeem, M. R. (2023). Implementation of various control methods for the efficient energy management in hybrid microgrid system. *Ain Shams Engineering Journal*, 14(5), 101961.

[14] Xiao, Yulong, et al. "Feasibility study: Economic and technical analysis of optimal configuration and operation of a hybrid CSP/PV/wind power cogeneration system with

energy storage." *Renewable Energy,* 225 (2024): 120273.

[15] Vendoti, Suresh, M. Muralidhar, and R. Kiranmayi. "Techno-economic analysis of off-grid solar/wind/biogas/biomass/fuel cell/battery system for electrification in a cluster of villages by HOMER software." *Environment, Development and Sustainability* 23.1 (2021): 351-372.

[16] Xiao, Y., Zou, C., Dong, M., Chi, H., Yan, Y., & Jiang, S. (2024). Feasibility study: Economic and technical analysis of optimal configuration and operation of a hybrid CSP/PV/wind power cogeneration system with energy storage. *Renewable Energy*, 225, 120273.

[17] Satapathy, S., & Naik, A. (2016). Social group optimization (SGO): a new population evolutionary optimization technique. *Complex & Intelligent Systems*, 2(3), 173-203.

[18] Naik, A., Satapathy, S. C., & Abraham, A. (2020). Modified Social Group Optimization—A meta-heuristic algorithm to solve short-term hydrothermal scheduling. *Applied Soft Computing*, 95, 106524.

Contribution of Individual Authors to the Creation of a Scientific Article (Ghostwriting Policy)

- Madhab Chandra Das carried out the Ideas; formulation, simulation, and optimization.
- Pritam Patel has implemented the Algorithm SGO and is responsible for the Statistics.
- Sarat Chandra Swain has Conducted a research and investigation process, specifically performing the experiments and data collection.
- Binay Kumar Nayak has Preparation, creation, and presentation of the published work, specifically writing the initial draft.

Sources of Funding for Research Presented in a Scientific Article or Scientific Article Itself

This research received no external funding.

Conflict of Interest

The authors have no conflicts of interest

Creative Commons Attribution License 4.0 (Attribution 4.0 International, CC BY 4.0)